University of Kent

Kent Academic Repository

Doheny, Patrick W., Stenning, Gavin G.B. and Saines, Paul J. (2025) *Magnetic and magnetocaloric properties of the two-dimensional Ln2(phthalate)3(H2O) (Ln = Gd-Dy) framework series.* Journal of Magnetism and Magnetic Materials . ISSN 0304-8853.

Downloaded from

https://kar.kent.ac.uk/110315/ The University of Kent's Academic Repository KAR

The version of record is available from

https://doi.org/doi:10.1016/j.jmmm.2025.173253

This document version

Publisher pdf

DOI for this version

Licence for this version

CC BY (Attribution)

Additional information

Versions of research works

Versions of Record

If this version is the version of record, it is the same as the published version available on the publisher's web site. Cite as the published version.

Author Accepted Manuscripts

If this document is identified as the Author Accepted Manuscript it is the version after peer review but before type setting, copy editing or publisher branding. Cite as Surname, Initial. (Year) 'Title of article'. To be published in ***Title of Journal*** , Volume and issue numbers [peer-reviewed accepted version]. Available at: DOI or URL (Accessed: date).

Enquiries

If you have questions about this document contact ResearchSupport@kent.ac.uk. Please include the URL of the record in KAR. If you believe that your, or a third party's rights have been compromised through this document please see our Take Down policy (available from https://www.kent.ac.uk/guides/kar-the-kent-academic-repository#policies).

Journal Pre-proofs

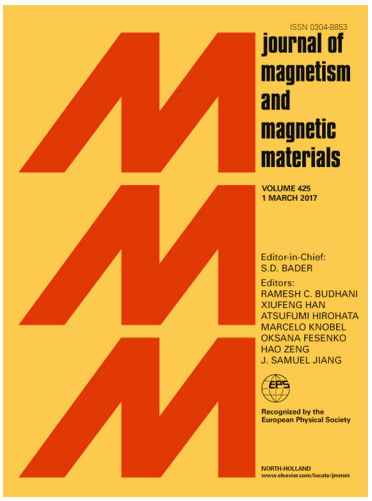

Magnetic and magnetocaloric properties of the two-dimensional Ln_2(phthalate)$_3$(H_2O) (Ln = Gd-Dy) framework series

Patrick W. Doheny, Gavin G.B. Stenning, Paul J. Saines

PII: S0304-8853(25)00485-8
DOI: https://doi.org/10.1016/j.jmmm.2025.173253
Reference: MAGMA 173253

To appear in: *Journal of Magnetism and Magnetic Materials*

Received Date: 19 February 2025
Revised Date: 16 April 2025
Accepted Date: 30 May 2025

Please cite this article as: P.W. Doheny, G.G.B. Stenning, P.J. Saines, Magnetic and magnetocaloric properties of the two-dimensional Ln_2(phthalate)$_3$(H_2O) (Ln = Gd-Dy) framework series, *Journal of Magnetism and Magnetic Materials* (2025), doi: https://doi.org/10.1016/j.jmmm.2025.173253

This is a PDF file of an article that has undergone enhancements after acceptance, such as the addition of a cover page and metadata, and formatting for readability, but it is not yet the definitive version of record. This version will undergo additional copyediting, typesetting and review before it is published in its final form, but we are providing this version to give early visibility of the article. Please note that, during the production process, errors may be discovered which could affect the content, and all legal disclaimers that apply to the journal pertain.

© 2025 The Author(s). Published by Elsevier B.V.

Magnetic and Magnetocaloric Properties of the Two-Dimensional $Ln_2(phthalate)_3(H_2O)$ (Ln = Gd-Dy) Framework Series

Patrick W. Doheny,[a] Gavin G. B. Stenning[b] and Paul J. Saines*[a]

[a] School of Chemistry and Forensic Science, University of Kent, Ingram Building, Canterbury, CT2 7NH, UK

[b] ISIS Neutron and Muon Source, STFC Rutherford Appleton Laboratory, Chilton, Didcot OX11 0QX, United Kingdom

* Corresponding author's email: P.Saines@kent.ac.uk

Abstract

The magnetic properties of a series of layered, two-dimensional $Ln_2(phth)_3(H_2O)$ materials (where Ln = Gd-Dy and phth = phthalate) metal-organic framework (MOF) materials have been examined to evaluate their potential as magnetocaloric materials. The $Gd_2(phth)_3(H_2O)$ material was found to exhibit the best performance of the series with a $-\Delta S_m^{max}$ of 16.3 J kg^{-1} K^{-1} for a magnetic field change of 5-0 T. Although modest compared to other Gd-based magnetocaloric frameworks, this material was notable for exhibiting its peak entropy change at 4 K. This contrasts with the majority of Gd-based magnetocaloric materials whose performance is usually optimised at 2 K (or lower) and found to rapidly decrease with increasing temperature and is attributed to the stronger magnetic interactions present in this material.

Keywords: Magnetocaloric; coordination framework; lanthanide; magnetism

Introduction

Quantum computing, spintronic, hydrogen liquefaction and medical imaging applications are all underpinned by the need for cooling to temperatures below 80 K.[1-5] Currently, cooling and refrigeration below 77 K (the boiling point of liquid nitrogen) is routinely achieved using liquid helium to reach temperatures down to 2 K while dilution refrigerators, utilising a mixture of ^{3}He and ^{4}He, can achieve even lower temperatures in the mK range. This highlights the dependence of low temperature cooling on liquid helium, a non-renewable resource that is becoming increasingly expensive and scarce with major sources currently dominated by two countries.[6] To combat this, the development of new materials capable of cooling to low temperatures without the need for liquid helium is an active area of research with the goals of developing cost and energy effective low temperature cooling methods and relieving the dependence on the finite resource of helium.

One method by which this may be achieved is by exploiting the magnetocaloric effect, a process where subjecting paramagnetic materials to a cycled magnetic field leads to a decrease in their temperature. This occurs *via* an entropically-driven solid-state cooling process arising from the loss of magnetic entropy upon alignment of spins with an external magnetic field (leading to heat absorption by the material) followed by the removal of this field which leads to an increase in magnetic entropy and subsequent cooling of the material.[7] The

magnetocaloric effect, first discovered in 1917,[8] has since enjoyed intense interest from both fundamental[9-11] and applied[12-14] areas of research in developing fully renewable low temperature cooling materials and devices. The dependence of the magnetocaloric effect on the magnetic entropy change under cycling of an external magnetic field has resulted in lanthanide-based materials becoming ideal candidates for magnetocaloric materials due to their large number of unpaired spins and subsequent large magnetic entropy changes. Both metal clusters[15-17] and oxides[18-20] have demonstrated impressive magnetocaloric properties such as the $Gd_3Ga_5O_{12}$ (GGG) material,[21] a material often employed as a benchmark to evaluate potential magnetocaloric materials. These material classes have different weaknesses with the metal clusters having low performance as a function of density, which increases the amount of material that must be exposed to the magnetic field, due to the bulky organic ligands used to isolate the clusters while metal oxides commonly adopt close-packed structures, limiting the ability to tune the dimensionality of their magnetic properties. Coordination polymers and Metal-Organic Frameworks (MOFs) are alternative classes of materials that offer the ability to systematically tailor magnetic properties by topological design targeting suppression of long-range magnetic order, rapid low-field magnetisation and high magnetic densities, all of which are difficult to achieve in other materials.[10, 22, 23] Lanthanide-based MOFs and coordination polymers have already shown impressive magnetocaloric performance such as hydroxides,[5, 24] carbonates,[9, 25, 26] formates,[27, 28] and oxalates[21, 29, 30] where the use of small organic or inorganic ligands leads to a structurally dense materials with a high concentration of magnetic ions.

This study details the investigation of the magnetocaloric properties of the $Ln_2(phth)_3(H_2O)$ (where Ln = Gd-Dy and phth = phthalate) series of MOFs which exhibit a structural topology of 2D Ln sheets bound by phthalate ligands to form layered 2D materials. While the structure of these phases, along with their La, Sm and Eu analogues, have been reported before alongside some optical measurements, the magnetic properties of this family have not yet been reported.[31-35] Herein, we focus on the later lanthanides due to their large magnetic moments, which offers the potential for greater magnetocaloric entropy changes.[10] We find that the $Gd_2(phth)_3(H_2O)$ compound exhibits the highest magnetocaloric entropy change of the three compounds reported in this work with an unusual increase in the temperature at which its maximum entropy change occurs with higher applied fields, which we associate with this compound likely having the strongest magnetic interactions.

Synthesis and Structure

The $Ln_2(phth)_3(H_2O)$ frameworks were synthesised following a combination of previously published procedures with modifications.[31, 32] The $LnCl_3{\cdot}xH_2O$ salt, phthalic acid and 1,2-bis(4-pyridyl)ethane were mixed in 10 mL of water and heated at 180 °C for 48 hr in a Teflon lined autoclave. After cooling to room temperature, colourless plate crystals suitable for single crystal X-ray diffraction analysis were harvested from the mother liquor and washed with water. These compounds were found to adopt structures consistent with the previous reports of the monoclinic $P2_1/c$ $Ln_2(phth)_3(H_2O)$ phases (adopted by Sm-Dy) with asymmetric units (Figures S1-S3) consisting of two Ln cations, three phthalate ligands and one water molecule. The structures were characterised by Ln^{3+} cations linked by phthalate ligands to form a layered, two-dimensional sheet topology along the *ac*-plane. The sheets consist of 1D Ln^{3+} chains that are linked by phthalate ligands to form an alternating arrangement of corner- and edge-sharing polyhedra. These 1D chains are further cross-linked by the carboxylate ligands of the phthalate ligands to yield 2D sheets of Ln^{3+} ions (Figure 1a) which also feature hydrogen bonding

between the coordinated water molecules and adjacent carboxylate groups. These sheets are stacked along the *b*-axis (Figure 1b) to form a layered structure of isolated 2D sheets of Ln^{3+} cations with aromatic rings capping the layers.

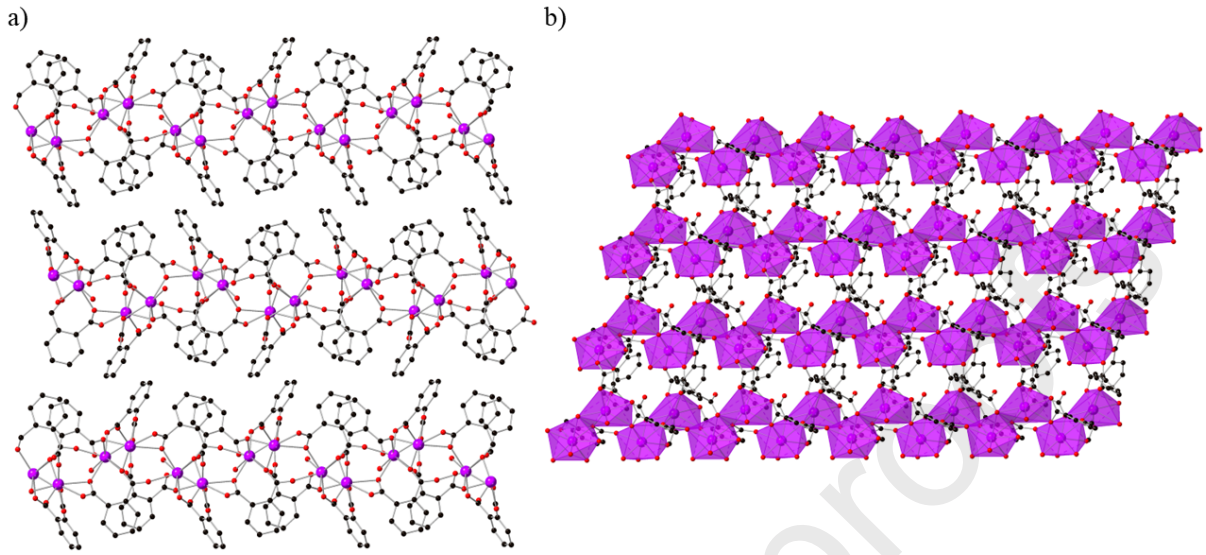

Figure 1. Crystal structure of the $Ln_2(phth)_3(H_2O)$ series showing a) the layered 2D sheets viewed along the *a*-axis and b) the 1D Ln^{3+} chains of alternating corner- and edge-sharing polyhedral cross-linked by phthalate ligands to form 2D sheets of Ln^{3+} cations viewed along the *b*-axis. Atom labelling: Ln = purple, O = red and C = black. The hydrogen atoms have been omitted for clarity.

Bulk powder samples of the $Ln_2(phth)_3(H_2O)$ frameworks were obtained by grinding the single crystals obtained from the solvothermal synthesis into a fine powder. Phase purity of the materials was assessed using powder X-ray diffraction with Le Bail extractions (Figures S4-S6) of the resulting powder diffraction patterns confirming the phase purity of the target compounds with the exception of a single impurity peak found in the $Dy_2(phth)_3(H_2O)$ pattern at low angle. Thermogravimetric analysis (Figures S7-S9) indicated gradual mass loss, consistent with evaporation of residual surface solvent, until 250 °C, where small sudden mass losses of 3.4% (Gd), 2.4% (Tb) and 2.7% (Dy) were observed. These mass losses were attributed to the loss of coordinated water molecules from the Ln^{3+} ions in the framework and were consistent with the molecular formulae determined from the single crystal X-ray diffraction (see Table S6 for comparisons of experimental and calculated mass losses). This loss of coordinated solvent was then followed by a larger mass loss around 400 °C, consistent with the decomposition of the organic ligand and the framework structures. Solid-state IR analysis (Figure S10) of the frameworks also indicated the presence of water in the framework structures with bands present at 3223, 3300 and 3449 cm^{-1} consistent with the OH stretches found in water.[36] Bands were also observed at 1043, 1084, 1148, 1165, 1352 and 1558 cm^{-1} in the spectra of all three materials that were consistent with those reported in reference 37 for the phthalate dianion, which is present in each of the framework structures.[37]

Magnetic Properties

Field-cooled (FC) and zero field-cooled (ZFC) magnetic susceptibility measurements of the $Ln_2(phth)_3(H_2O)$ materials were carried out in a 1000 Oe field over a 2-300 K temperature range. The FC and ZFC data for all three materials (Figures 2, S11 and S12) did not show any evidence of long-range magnetic ordering down to 2 K.

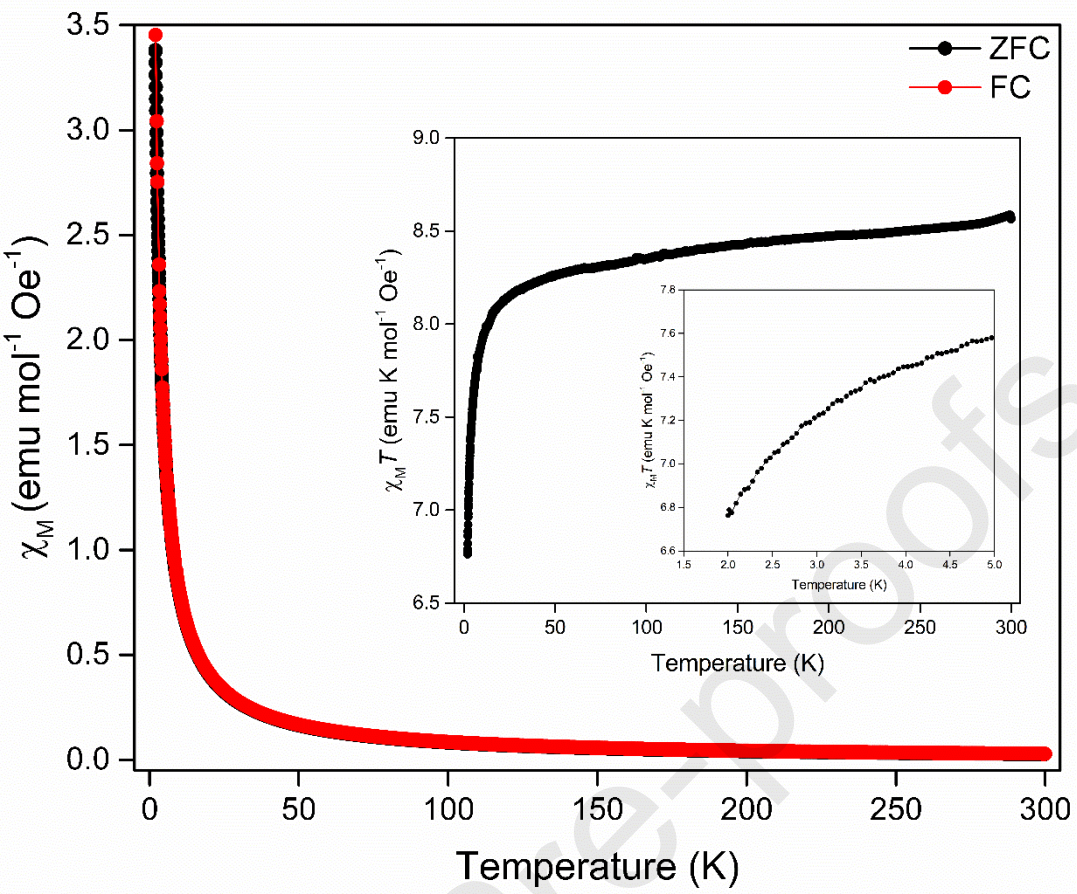

Figure 2. ZFC and FC magnetic susceptibility of $Gd_2(phth)_3(H_2O)$ in a 1000 Oe field over a 2-300 K temperature range. Inserts: $\chi_M T$ plots over a 2-5 and 2-300K temperature range.

Fitting of the Curie-Weiss law to the data (Figures S13-S15), from 2-300 K, yielded small, negative Weiss temperatures (Table 1) that suggested weak antiferromagnetic interactions for all three phases; it should be noted that there may also be contributions to this from low temperature crystal field effects for the Tb and Dy phases but, crucially, not Gd whose $4f^7$ configuration lacks any orbital angular momentum. The effective magnetic moments (μ_{eff}) of all three materials were also found to be broadly consistent with the values predicted for trivalent lanthanide ions given by the Russell-Saunders coupling scheme.[38]

Table 1. Weiss temperatures, effective and theoretical magnetic moments of the $Ln_2(phth)_3(H_2O)$ series.

Ln	Weiss Temperature (K)	Effective μ_{eff} (μ_B)	Theoretical μ_{eff} (μ_B)
Gd	-3.59(4)	8.4778(8)	7.94
Tb	-3.44(1)	9.8658(3)	9.72
Dy	-1.92(1)	11.1062(1)	10.65

The low-temperature evolution of $\chi_M T$ was consistent with antiferromagnetic coupling with each material showing a decrease in $\chi_M T$ with decreasing temperature. This decrease was most rapid for the Gd material with sustained decreases below 300 K while the $\chi_M T$ of the Dy phase only began to decrease rapidly below 50 K and was more gradual. This was consistent with the antiferromagnetic interactions being greatest in the Gd material and weakest in the Dy as suggested by their Weiss temperatures. These are presumably within the layers of these compounds given the Ln cations in different layers are separated by more than 10 Å, although it is not clear whether they are restricted to the O bridged 1D chains of Ln cations or the aromatic linkers also facilitate significant magnetic communication. Given the changes in magnetic superexchange distances and angles (Tables S4-S5) across all three materials is very modest, the differences in magnetic properties observed across the series is attributed to the difference in the number of unpaired electrons.

Isothermal magnetisation measurements at 2 K (Figure 3) showed that all three materials reached saturation magnetisation (M_{sat}) at fields of 50 kOe with the Gd phase reaching the highest M_{sat} value followed by the Dy and Tb materials. The Tb and Dy materials were found to magnetise rapidly such that the magnetisation only increased incrementally at fields > 10 kOe while the Gd phase underwent a much more gradual magnetisation such that saturation was reached only around 40 kOe.

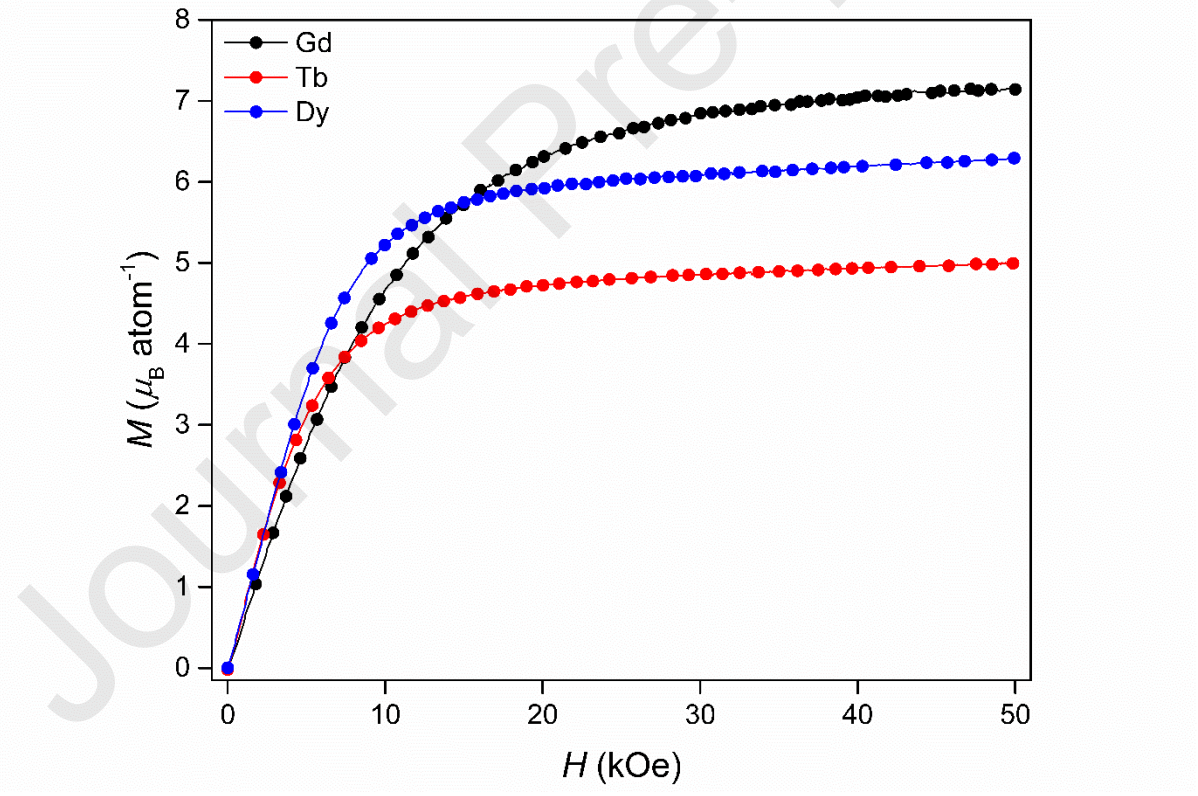

Figure 3. Isothermal magnetisation curves of the $Ln_2(phth)_3(H_2O)$ series at 2 K.

It is known that the magnetic anisotropy exhibited by powder samples can be inferred from the magnitude of its M_{sat} compared to the predicted values for Heisenberg and Ising spin systems given by $g_J J$ and $g_J J/2$ respectively.[9, 18, 39, 40] Comparing the predicted and experimental M_{sat} values (Table 2) suggested that the Gd material acts as a Heisenberg spin system while the

M_{sat} values of the Tb and Dy compounds are more consistent with greater magnetic anisotropy, although both values are slightly higher than those expected for Ising systems. This may suggest the Tb and Dy compounds deviate from pure Ising behaviour.

Table 2. Experimental saturation magnetisation (M_{sat}) values and predicted values for lanthanide Heisenberg and Ising spin systems.

Ln	M_{sat} (μ_B atom^{-1})	$g_J J$	$g_J J/2$
Gd	7.16	7	3.5
Tb	5.00	9	4.5
Dy	6.29	10	5

Magnetocaloric Properties

The magnetocaloric properties of the $Ln_2(phth)_3(H_2O)$ materials were evaluated using the Maxwell relation $\Delta S_m(T) = \int[\partial M(T,B)/\partial T]_B \, dB$ to calculate the magnetic entropy changes (ΔS_m) between 2-10 K and magnetic field changes between 0 and 1-5 T (see Figures S16-S18) for magnetisation data from which these are obtained). Despite being an indirect means of evaluating magnetocaloric properties, it has been previously shown that the ΔS_m values calculated using this method are in good agreement with those calculated from more direct heat capacity measurements.[25, 28] For changes of ΔB = 1-0 T (Figure S19), all three materials (Table 3) showed similar maximum entropy changes, $-\Delta S_m^{max}$, with the Gd phase achieving the highest of these modest changes of 3.5 J kg^{-1} K^{-1} at 2 K. The entropy changes decrease rapidly with increasing temperature.

Table 3. Maximum entropy changes ($-\Delta S_m^{max}$) and peak temperatures (T_{max}) of the $Ln_2(phth)_3(H_2O)$ series at different field changes.

	ΔB = 1-0 T		ΔB = 2-0 T		ΔB = 5-0 T	
Ln	T_{max} (K)	$-\Delta S_m^{max}$ (J kg^{-1} K^{-1})	T_{max} (K)	$-\Delta S_m^{max}$ (J kg^{-1} K^{-1})	T_{max} (K)	$-\Delta S_m^{max}$ (J kg^{-1} K^{-1})
Gd	2	3.5	3	7.73	4	16.3
Tb	2	3.3	2	4.90	4	6.0

Journal Pre-proofs

Dy	2	3.3	2	5.16	4	6.4

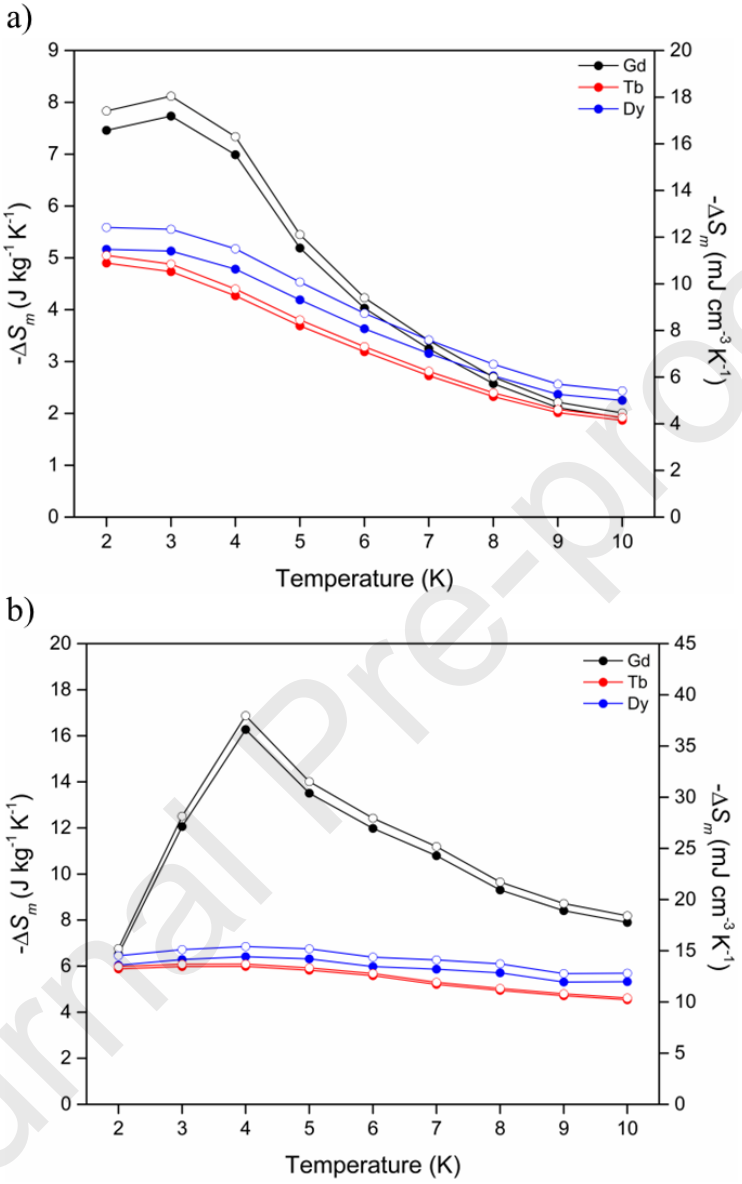

Figure 4. Magnetic entropy changes of the $Ln_2(phth)_3(H_2O)$ series for a) ΔB = 2-0 T and b) ΔB = 5-0 T. The filled and open symbols denote mass and volumetric entropy units respectively.

Interestingly, for ΔB = 2-0 T (Figure 4a), a shift of the $-\Delta S_m^{max}$ and associated T_{max} is observed for the Gd material to 7.7 J kg^{-1} K^{-1} at 3 K alongside a much more gradual decrease in entropy change with increasing temperature relative to the Tb and Dy phases; the later two compounds retain their respective T_{max} at 2 K although the Dy material's decrease with increasing temperature is more modest. At high field changes of ΔB = 5-0 T (Figure 4b), this increase in $-\Delta S_m^{max}$ and T_{max} for the Gd phase is much more pronounced with a $-\Delta S_m^{max}$ of 16.3 J kg^{-1} K^{-1} at 4 K. There is little change in $-\Delta S_m$ with temperature for the Tb and Dy materials. In comparing the $Ln_2(phth)_3(H_2O)$ series to other magnetocaloric materials, the best performing member of the series, $Gd_2(phth)_3(H_2O)$, recorded a maximum entropy change of 16.3 J kg^{-1} K^{-}

^{1} for a 5-0 T field change at 4 K. This is slightly less than half the entropy change of ~ 35 J kg^{-1} K^{-1} obtained from the GGG material, a benchmark magnetocaloric material, for the same field change.[21, 24] Despite this, we note that the GGG material's entropy changes tend to be maximised at 2 K or lower so the $Gd_2(phth)_3(H_2O)$ phase's superior performance at 4 K (relative to its performance at 2 K) is notable for a Gd-based magnetocaloric.

The Gd material's increase in $-\Delta S_m$ up to 4 K for a 5-0 T field change is unusual as Gd-based magnetocaloric materials typically exhibit a sustained decrease in $-\Delta S_m$ with increasing temperature above 2 K. Amongst coordination framework materials, such behaviour is usually associated with the more anisotropic Tb, Dy or Ho phases.[5, 9, 27] That this behaviour is seen in the Gd analogue in this compound is likely linked to it appearing to have the strongest magnetic interactions amongst the compounds examined in this study, although direct characterisation of the magnetic interactions on the atomic scale would be required to understand this in more details. This is complicated by Gd being a very high neutron absorber making neutron scattering studies, as usually used to study magnetic coupling on the atomic scale, extremely difficult.

Conclusions

This study has examined the magnetic and magnetocaloric properties of three 2D $Ln_2(phth)_3(H_2O)$ materials (where Ln = Gd-Dy) over a 2-10 K temperature range. The magnetic entropy changes of this isostructural series were characterised over an applied magnetic field range of 1-5 T with the $Gd_2(phth)_3(H_2O)$ framework proving to be the best performing material in all cases. Notably, the temperature at which the Gd material's $-\Delta S_m^{max}$ occurs gradually increases with increasing applied fields reaching 16.3 J kg^{-1} K^{-1} at 4 K. This contrasts with the more typically observed rapid decrease in $-\Delta S_m$ with increasing temperature above 2 K in Gd-based magnetocaloric materials. Although this behaviour is more commonly observed with magnetically anisotropic lanthanides such as Tb, Dy or Ho, it is attributed to the relatively strong magnetic interactions present in the $Gd_2(phth)_3(H_2O)$ material.

Experimental

Materials. All reagents and solvents were obtained from commercial sources and were used without further purification unless otherwise stated.

Framework synthesis. The $Ln_2(phth)_3(H_2O)$ frameworks were synthesised following a combination of previously published procedures with modifications.[31, 32]

$Gd_2(phth)_3(H_2O)$. $GdCl_3 \cdot 6H_2O$ (400 mg, 1.08 mmol), benzene-1,2-dicarboxylic acid (176 mg, 1.06 mmol) and 1,2-bis(4-pyridyl)ethane (98 mg, 0.53 mmol) were dissolved in water (10 mL) with the resulting solution sealed in a 25 mL Teflon-lined autoclave and heated at 180 °C for 48 h. After cooling to room temperature, the mixture was filtered and the solid washed with water and left to air dry to yield the framework as a white powder (24 mg, 0.03 mmol, 5%). Elemental analysis for $C_{24}H_{14}O_{13}Gd_2$: C 34.95%, H 1.71%. Found: C 34.56%, H 1.09%.

$Tb_2(phth)_3(H_2O)$. $TbCl_3 \cdot 6H_2O$ (405 mg, 1.08 mmol), benzene-1,2-dicarboxylic acid (176 mg, 1.06 mmol) and 1,2-bis(4-pyridyl)ethane (98 mg, 0.53 mmol) were dissolved in water (10 mL) with the resulting solution sealed in a 25 mL Teflon-lined autoclave and heated at 180 °C for 48 h. After cooling to room temperature, the mixture was filtered and the solid washed with water and left to air dry to yield the framework as a white powder (28 mg, 0.03 mmol, 6%). Elemental analysis for $C_{24}H_{14}O_{13}Tb_2$: C 34.81%, H 1.70%. Found: C 34.47%, H 1.35%.

$Dy_2(phth)_3(H_2O)$. $DyCl_3 \cdot 6H_2O$ (407 mg, 1.08 mmol), benzene-1,2-dicarboxylic acid (176 mg, 1.06 mmol) and 1,2-bis(4-pyridyl)ethane (98 mg, 0.53 mmol) were dissolved in water (10 mL) with the resulting solution sealed in a 25 mL Teflon-lined autoclave and heated at 180 °C for 48 h. After cooling to room temperature, the mixture was filtered and the solid washed with water and left to air dry to yield the framework as a white powder (36 mg, 0.04 mmol, 8%). Elemental analysis for $C_{24}H_{14}O_{13}Dy_2$: C 34.51%, H 1.69%. Found: C 34.30%, H 1.21%.

Physical Characterisation and Instrumentation

Thermogravimetric Analysis (TGA). TGA analysis was performed using a Netzsch STA 409 PC thermal analyser performed over a 25-800 °C min^{-1} temperature range at a ramp rate of 10 °C min^{-1} under an atmosphere of compressed air.

Single Crystal X-ray Diffraction. Single-crystal X-ray diffraction was performed using a Rigaku Oxford Supernova diffractometer equipped with an Oxford Cryosystems cryostream, an Atlas S2 CCD detector, and employing Mo Kα radiation generated using a sealed X-ray tube. All data was integrated within the CrysAlisPro software suite[41] with a face indexed absorption correction applied to the data of each collection. The structures were solved using SHELXT[42] with structural refinements carried out using SHELXL-2018/3[43] within the Olex2 graphical user interface.[44] All nonhydrogen atoms were refined anisotropically with the hydrogen atoms placed at calculated positions using a riding model. Crystallographic data are given in Tables S1−S3 and the CIFs have been deposited with the CCDC under deposition numbers CCDC 2388354-2388356.

Powder X-ray Diffraction (PXRD). PXRD patterns were collected using a PANalytical X'Pert Pro diffractometer producing Cu-Kα (λ = 1.5406 Å) radiation and equipped with a solid-state X'Celerator detector. All samples were finely ground prior to analysis and mounted on silicon zero background plates. The powder patterns of all materials were analysed using the GSAS-II program[45] with phase purity assessed using the Le Bail method.[46]

Magnetometry. DC magnetic susceptibility and magnetisation measurements were performed using a Quantum Design MPMS SQUID magnetometer with samples sealed inside a gelatin capsule that was mounted inside a plastic straw with a uniform diamagnetic background. Zero-field cooled (ZFC) and field-cooled (FC) magnetic susceptibility measurements were performed over a 2-300 K temperature range under an applied magnetic field of 1000 Oe. Isothermal magnetisation data was acquired over a 2-10 K temperature range under applied fields ranging from 0-5 T.

Conflicts of Interest

There are no conflicts to declare.

Data Availability Statement

Data for this article, including powder diffraction, TGA and magnetometry measurements are available at the Kent Data Repository at https://data.kent.ac.uk/id/eprint/539. Crystallographic data for all compounds have been deposited with the CCDC under deposition numbers CCDC 2388354-2388356.

Acknowledgements

We would like to thank the Engineering and Physical Sciences Research Council (EPSRC) for funding this research via grants EP/T027886/1.

Author Contributions

Investigation and formal analysis was primarily carried out by PWD under the supervision of PJS and with assistance from GBGS for physical property measurements. The project was conceptualized by PJS who also led on the funding acquisition. Data validation and visualisation was carried out by PWD and PJS. The manuscript was written by PWD with all authors contributing to its development *via* reviewing and editing.

References

[1] T.D. Ladd, F. Jelezko, R. Laflamme, Y. Nakamura, C. Monroe, J.L. O'Brien, Quantum computers, Nature, 464 (2010) 45-53, 10.1038/nature08812.

[2] A. Hirohata, K. Yamada, Y. Nakatani, I.-L. Prejbeanu, B. Diény, P. Pirro, B. Hillebrands, Review on spintronics: Principles and device applications, J. Magn. Magn. Mater., 509 (2020) 166711, https://doi.org/10.1016/j.jmmm.2020.166711.

[3] L. Gyongyosi, S. Imre, A Survey on quantum computing technology, Comput. Sci. Rev., 31 (2019) 51-71, https://doi.org/10.1016/j.cosrev.2018.11.002.

[4] M. van der Spek, C. Banet, C. Bauer, P. Gabrielli, W. Goldthorpe, M. Mazzotti, S.T. Munkejord, N.A. Røkke, N. Shah, N. Sunny, D. Sutter, J.M. Trusler, M. Gazzani, Perspective on the hydrogen economy as a pathway to reach net-zero CO_2 emissions in Europe, Energy Environ. Sci., 15 (2022) 1034-1077, 10.1039/D1EE02118D.

[5] P.W. Doheny, J. Chen, T. Gruner, F.M. Grosche, P.J. Saines, $Dy(OH)_3$: a paramagnetic magnetocaloric material for hydrogen liquefaction, J. Mater. Chem. A, 11 (2023) 26474-26480, 10.1039/D3TA05358J.

[6] A. Cho, Helium-3 Shortage Could Put Freeze On Low-Temperature Research, Science, 326 (2009) 778-779, doi:10.1126/science.326_778.

[7] A. Smith, Who discovered the magnetocaloric effect?, Eur. Phys. J. H, 38 (2013) 507-517, 10.1140/epjh/e2013-40001-9.

[8] P. Weiss, A. Piccard, Le phénomène magnétocalorique, J. Phys. Theor. Appl., 7 (1917) 103-109,

[9] R.J.C. Dixey, P.J. Saines, Optimization of the Magnetocaloric Effect in Low Applied Magnetic Fields in $LnOHCO_3$ Frameworks, Inorg. Chem., 57 (2018) 12543-12551, 10.1021/acs.inorgchem.8b01549.

[10] M. Falsaperna, P.J. Saines, Development of magnetocaloric coordination polymers for low temperature cooling, Dalton Trans., 51 (2022) 3394-3410, 10.1039/D1DT04073A.

[11] M. Wali, R. Skini, M. Khlifi, E. Dhahri, E.K. Hlil, A giant magnetocaloric effect with a tunable temperature transition close to room temperature in Na-deficient $La_{0.8}Na_{0.2-x}\square_xMnO_3$ manganites, Dalton Trans., 44 (2015) 12796-12803, 10.1039/C5DT01254F.

[12] J. Lyubina, Magnetocaloric materials for energy efficient cooling, J. Phys. D: Appl. Phys., 50 (2017) 053002, 10.1088/1361-6463/50/5/053002.

[13] A. Kitanovski, Energy Applications of Magnetocaloric Materials, Adv. Energy Mater., 10 (2020) 1903741, https://doi.org/10.1002/aenm.201903741.

[14] J.Y. Law, L.M. Moreno-Ramírez, Á. Díaz-García, V. Franco, Current perspective in magnetocaloric materials research, J. Appl. Phys., 133 (2023), 10.1063/5.0130035.

[15] H.-J. Lun, L. Xu, X.-J. Kong, L.-S. Long, L.-S. Zheng, A High-Symmetry Double-Shell $Gd_{30}Co_{12}$ Cluster Exhibiting a Large Magnetocaloric Effect, Inorg. Chem., 60 (2021) 10079-10083, 10.1021/acs.inorgchem.1c00993.

[16] N.-F. Li, Q.-F. Lin, X.-M. Luo, J.-P. Cao, Y. Xu, Cl–-Templated Assembly of Novel Peanut-like $Ln_{40}Ni_{44}$ Heterometallic Clusters Exhibiting a Large Magnetocaloric Effect, Inorg. Chem., 58 (2019) 10883-10889, 10.1021/acs.inorgchem.9b01261.

[17] J.-B. Peng, X.-J. Kong, Q.-C. Zhang, M. Orendáč, J. Prokleška, Y.-P. Ren, L.-S. Long, Z. Zheng, L.-S. Zheng, Beauty, Symmetry, and Magnetocaloric Effect—Four-Shell Keplerates with 104 Lanthanide Atoms, J. Am. Chem. Soc, 136 (2014) 17938-17941, 10.1021/ja5107749.

[18] P. Mukherjee, S.E. Dutton, Enhanced Magnetocaloric Effect from Cr Substitution in Ising Lanthanide Gallium Garnets $Ln_3CrGa_4O_{12}$ (Ln = Tb, Dy, Ho), Adv. Funct. Mater. , 27 (2017) 1701950, https://doi.org/10.1002/adfm.201701950.

[19] A. Barman, S. Kar-Narayan, D. Mukherjee, Caloric Effects in Perovskite Oxides, Adv. Mater. Interfaces, 6 (2019) 1900291, https://doi.org/10.1002/admi.201900291.

[20] N.K. Chogondahalli Muniraju, R. Baral, Y. Tian, R. Li, N. Poudel, K. Gofryk, N. Barišić, B. Kiefer, J.H. Ross, H.S. Nair, Magnetocaloric Effect in a Frustrated Gd-Garnet with No Long-Range Magnetic Order, Inorg. Chem., 59 (2020) 15144-15153, 10.1021/acs.inorgchem.0c02074.

[21] M. Falsaperna, G.B.G. Stenning, I. da Silva, P.J. Saines, Magnetocaloric $Ln(HCO_2)(C_2O_4)$ frameworks: synthesis, structure and magnetic properties, J. Mater. Chem. C, 9 (2021) 13209-13217, 10.1039/D1TC01831K.

[22] M. Kurmoo, Magnetic metal–organic frameworks, Chem. Soc. Rev., 38 (2009) 1353-1379, 10.1039/B804757J.

[23] G. Mínguez Espallargas, E. Coronado, Magnetic functionalities in MOFs: from the framework to the pore, Chem. Soc. Rev., 47 (2018) 533-557, 10.1039/C7CS00653E.

[24] Y. Yang, Q.-C. Zhang, Y.-Y. Pan, L.-S. Long, L.-S. Zheng, Magnetocaloric effect and thermal conductivity of $Gd(OH)_3$ and $Gd_2O(OH)_4(H_2O)_2$, Chem. Commun., 51 (2015) 7317-7320, 10.1039/C5CC01254F.

[25] Y.-C. Chen, L. Qin, Z.-S. Meng, D.-F. Yang, C. Wu, Z. Fu, Y.-Z. Zheng, J.-L. Liu, R. Tarasenko, M. Orendáč, J. Prokleška, V. Sechovský, M.-L. Tong, Study of a magnetic-cooling material $Gd(OH)CO_3$, J. Mater. Chem. A, 2 (2014) 9851-9858, 10.1039/C4TA01646G.

[26] Q. Tang, Y.-L. Yang, N. Zhang, Z. Liu, S.-H. Zhang, F.-S. Tang, J.-Y. Hu, Y.-Z. Zheng, F.-P. Liang, A Multifunctional Lanthanide Carbonate Cluster Based Metal–Organic Framework Exhibits High Proton Transport and Magnetic Entropy Change, Inorg. Chem., 57 (2018) 9020-9027, 10.1021/acs.inorgchem.8b01023.

[27] P.J. Saines, J.A.M. Paddison, P.M.M. Thygesen, M.G. Tucker, Searching beyond Gd for magnetocaloric frameworks: magnetic properties and interactions of the $Ln(HCO_2)_3$ series, Mater. Horiz., 2 (2015) 528-535, 10.1039/C5MH00113G.

[28] G. Lorusso, J.W. Sharples, E. Palacios, O. Roubeau, E.K. Brechin, R. Sessoli, A. Rossin, F. Tuna, E.J.L. McInnes, D. Collison, M. Evangelisti, A Dense Metal–Organic Framework for Enhanced Magnetic Refrigeration, Adv. Mater., 25 (2013) 4653-4656, https://doi.org/10.1002/adma.201301997.

[29] R. Sibille, E. Didelot, T. Mazet, B. Malaman, M. François, Magnetocaloric effect in gadolinium-oxalate framework $Gd_2(C_2O_4)_3(H_2O)_6{\cdot}(0.6H_2O)$, APL Mater., 2 (2014), 10.1063/1.4900884.

[30] M.N. Akhtar, Y.-C. Chen, M.A. AlDamen, M.-L. Tong, 3D oxalato-bridged lanthanide(iii) MOFs with magnetocaloric, magnetic and photoluminescence properties, Dalton Trans., 46 (2017) 116-124, 10.1039/C6DT03843C.

[31] S.F. Lush, F.M. Shen, Poly[[aquatris([mu]4-benzene-1,2-dicarboxylato)dilanthanum(III)] hemihydrate], Acta Cryst., E67 (2011) m1370-m1371, doi:10.1107/S1600536811036282.

[32] Y. Wan, L. Jin, K. Wang, L. Zhang, X. Zheng, S. Lu, Hydrothermal synthesis and structural studies of novel 2-D lanthanide coordination polymers with phthalic acid, New J. Chem., 26 (2002) 1590-1596, 10.1039/B206280C.

[33] Y.-S. Song, B. Yan, Z.-X. Chen, A novel unexpected two-dimensional layer-like luminescent dysprosium coordination polymer $[Dy_2(phth)_3H_2O]_n$ by hydrothermal synthesis, Can. J. Chem., 82 (2004) 1745-1751, 10.1139/v04-148.

[34] Z.-R. Meng, Q.-Z. Zhang, X.-Y. Wu, L.-J. Chen, C.-Z. Lu, Poly[aquabis([mu]4-benzene-1,2-dicarboxylato)([mu]3-benzene-1,2-dicarboxylato)digadolinium(III)], Acta Cryst., E62 (2006) m1033-m1035, https://doi.org/10.1107/S1600536806011433.

[35] X. Li, M.-Q. Zha, X.-W. Wang, R. Cao, Novel topological nets of lanthanide metal-organic frameworks based on dicarboxylate ligands, Inorg. Chim. Acta, 362 (2009) 3357-3363, https://doi.org/10.1016/j.ica.2009.03.017.

[36] D. Coker, J. Reimers, R. Watts, The Infrared Absorption Spectrum of Water, Aust. J. Phys., 35 (1982) 623-638, https://doi.org/10.1071/PH820623.

[37] J.S. Loring, M. Karlsson, W.R. Fawcett, W.H. Casey, Infrared spectra of phthalic acid, the hydrogen phthalate ion, and the phthalate ion in aqueous solution, Spectrochim. Acta, A57 (2001) 1635-1642, https://doi.org/10.1016/S1386-1425(01)00391-2.

[38] H.N. Russell, F.A. Saunders, New Regularities in the Spectra of the Alkaline Earths, Astrophys. J., 61 (1925) 38, 10.1086/142872.

[39] P.W. Doheny, S.J. Cassidy, P.J. Saines, Investigations of the Magnetocaloric and Thermal Expansion Properties of the $Ln_3(adipate)_{4.5}(DMF)_2$ (Ln = Gd–Er) Framework Series, Inorg. Chem., 61 (2022) 4957-4964, 10.1021/acs.inorgchem.1c03688.

[40] R.J.C. Dixey, F. Orlandi, P. Manuel, P. Mukherjee, S.E. Dutton, P.J. Saines, Emergent magnetic order and correlated disorder in formate metal-organic frameworks, Philos. Trans. R. Soc., A, 377 (2019) 20190007, 10.1098/rsta.2019.0007.

[41] CrysAlisPro, Rigaku Oxford Diffraction Ltd, Yarnton, Oxfordshire, England, 2019.

[42] G. Sheldrick, SHELXT - Integrated space-group and crystal-structure determination, Acta Cryst., A71 (2015) 3-8, doi:10.1107/S2053273314026370.

[43] G. Sheldrick, Crystal structure refinement with SHELXL, Acta Cryst., C71 (2015) 3-8, doi:10.1107/S2053229614024218.

[44] O.V. Dolomanov, L.J. Bourhis, R.J. Gildea, J.A.K. Howard, H. Puschmann, OLEX2: a complete structure solution, refinement and analysis program, J. Appl. Cryst., 42 (2009) 339-341, doi:10.1107/S0021889808042726.

[45] B.H. Toby, R.B. Von Dreele, GSAS-II: the genesis of a modern open-source all purpose crystallography software package, J. Appl. Cryst., 46 (2013) 544-549, doi:10.1107/S0021889813003531.

[46] A. Le Bail, H. Duroy, J.L. Fourquet, Ab-initio structure determination of $LiSbWO_6$ by X-ray powder diffraction, Mat. Res. Bull., 23 (1988) 447-452, https://doi.org/10.1016/0025-5408(88)90019-0.

Highlights

- The magnetic properties of the $Ln_2(phthalate)_3(H_2O)$ (Ln = Gd, Tb and Dy) were explored
- The Gd analogue has the best performance as a magnetocaloric, which unusually for Gd is maximised at 4 K rather than below 2 K
- This is attributed to the stronger interactions in this compounds being stronger than other members of the series
- This highlights a route forward to developing more sustainable magnetocalorics for replacing cooling using liquid He

Journal Pre-proofs